Synthesis, Ligand Binding, and QSAR (CoMFA and Classical) Study of 3β-(3′-Substituted phenyl)-, 3β-(4′-Substituted phenyl)-, and 3β-(3′,4′-Disubstituted phenyl)tropane-2β-carboxylic Acid Methyl Esters

F. Ivy Carroll,[*,†] S. Wayne Mascarella,[†] Michael A. Kuzemko,[†] Yigong Gao,[†] Philip Abraham,[†] Anita H. Lewin,[†] John W. Boja,[‡] and Michael J. Kuhar[‡]

Chemistry and Life Sciences, Research Triangle Institute, P.O. Box 12194, Research Triangle Park, North Carolina 27709, and Neuroscience Branch, Addiction Research Center, National Institute on Drug Abuse, Baltimore, Maryland 21224

Received April 18, 1994[®]

Several new 3β-(4′-substituted phenyl)-, 3β-(3′-substituted phenyl)-, and 3β-(3′,4′-disubstituted phenyl)tropane-2β-carboxylic acid methyl esters were prepared and assayed for inhibition of [³H]WIN 35,428 binding to the dopamine transporter. The 3β-(3′,4′-dichloro) and 3β-(4′-chloro-3′-methyl) analogues (**2w** and **2y**; RTI-111 and RTI-112, respectively) with IC$_{50}$ values of 0.79 and 0.81 nM showed the highest affinity. The contributions of quantitative structure–activity relationship (QSAR) models derived from the classical and comparative molecular field analysis (CoMFA) approaches to rational drug design were examined. CoMFA models were derived using steric and electrostatic potentials with SYBYL default values while the classical models were derived from π and MR parameters. Using a 12-compound training set, both models were used for predicting the binding affinity of compounds both inside and outside the training set. The CoMFA study provided new insight into the steric and electrostatic factors influencing binding to the DA transporter and provided additional support for our original finding that CoMFA is useful in predicting and designing new compounds for study. The classical QSAR models, which were easier to obtain, suggest that the distribution property (π) of the compounds is an important factor. Overall, the SAR, CoMFA, and conventional QSAR studies elaborated some features of the cocaine binding site pharmacophore and provided useful predictive information.

Introduction

In order to understand the mechanism related to the addictive properties of cocaine, it was necessary to identify the molecular site where this drug interacts to produce its initial physiological effects. (−)-Cocaine (1) has several sites of action in the central nervous system of rodents and nonhuman primates, as well as in the human brain.[1-5] Of these, the dopaminergic pathway has been implicated in the reinforcing properties of (−)-cocaine.[6,7] Thus, Ritz et al.[8] and Bergman et al.[9] found a significant correlation between the rank order for maintaining drug self-administration of various (−)-cocaine-related drugs and their potency at the dopamine transporter cocaine binding site. The biological relevance of this binding site was also supported by the finding that it is highly stereoselective, with natural (−)-cocaine (1) being 60–600 times more potent than its seven stereoisomers.[10] Even though it has been known for some time that (−)-cocaine inhibits the reuptake of dopamine, the exact mechanism of this inhibition is still not fully understood. Recently much research has been directed toward this problem.[6]

1
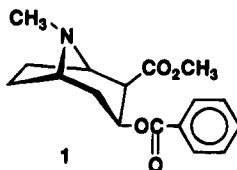
Although the dopamine transporter has been cloned and expressed, its three-dimensional structure is

unknown.[11-14] However, some information about the structural characteristics of the cocaine binding site has been obtained from structure–activity relationship (SAR) studies.[6] Much of the information has come from studies on the structurally relatively rigid 3β-phenyltropane-2β-carboxylic acid methyl ester **2a** (WIN 35,-065-2) class of compounds.[6,15-24] In addition to the absolute stereochemistry found in **2a**, the tropane nitrogen, a 2β-substituent, and a 3β-aryl group are required for high-affinity binding to the DA transporter. However, we, and others, have found that binding affinities were highly dependent upon the substituents on the phenyl ring.[17,18,23] We have also reported the use of comparative molecular field analysis (CoMFA) for the development of a predictive model for inhibition of radioligand binding to the dopamine transporter.[17] Since this report, Good et al.[25] conducted QSAR studies on the same data set using a molecular similarity matrices approach, and Srivastava and Crippin[26] reported a three-dimensional Voronoi site modeling approach to a different set of cocaine analogues.

The present study reports the synthesis of several new analogues and binding data for 13 new ring-substituted analogues of **2a**. In addition, the original CoMFA model[17] has been updated, a classical QSAR model was developed, and both models were used to predict the binding affinity of the 13 new analogues. In order to further optimize the cocaine binding site pharmacophore, CoMFA and classical QSAR models, using all 25 analogues, have been developed. A part of this work was described in a preliminary communication.[23] Some of the new analogues described in this preliminary report have subsequently been synthesized and studied by Meltzer et al.[18]

---

† Research Triangle Institute.
‡ National Institute on Drug Abuse.

Table 1. Potencies of 3β-(Substituted phenyl)tropane-2β-carboxylic Acid Methyl Esters in Inhibition of 0.5 nM [^{3}H]WIN 35428

compd	X	Y	IC$_{50}$ (nM)^a
2a	H	H	23 ± 5.0
2b	F	H	13.9 ± 1.4
2c	Cl	H	1.12 ± 0.10
2d	Br	H	1.69 ± 0.23
2e	NO$_2$	H	13.1 ± 0.1
2f	NH$_2$	H	9.84 ± 0.29
2g	CH$_3$CONH	H	64.2 ± 2.6
2h	C$_2$H$_5$CONH	H	121 ± 2.7
2i	C$_2$H$_5$OCONH	H	316 ± 48
2j	CH$_3$	H	1.71 ± 0.31
2k	I	H	1.26 ± 0.04
2l	CF$_3$	H	13.0 ± 2.2
2m	CH$_3$O	H	9.2 ± 1.3
2n	N$_3$	H	2.12 ± 0.13
2o	C$_2$H$_5$	H	55 ± 2.1
2p	OH	H	12.1 ± 0.86
2q	(CH$_3$)$_3$Sn	H	144 ± 37
2r	H	F	16.4 ± 2.8
2s	H	Cl	6.27 ± 1.2
2t	H	I	26.1 ± 1.7
2u	NH$_2$	I	1.35 ± 0.11
2v	NH$_2$	Br	3.91 ± 0.59
2w	Cl	Cl	0.79 ± 0.08
2x	F	CH$_3$	2.95 ± 0.58
2y	Cl	CH$_3$	0.81 ± 0.05

^{a} Mean ± standard error of at least four experiments performed in triplicate.

Chemistry

Since the aim of the present study was to investigate the effect of aromatic substitution of **2a** on inhibition of binding of [^{3}H]WIN 35,428 to the DA transporter, the study was restricted to 3β-(substituted phenyl)tropane-2β-carboxylic acid methyl esters **2**. Table 1 lists the compounds that were used in the present study. The syntheses of compounds **2a-o**, **2q**, and **2u** were reported in earlier publications.[17,27,28] Since we noted that compounds **2f** and **2h** were highly hygroscopic, new samples of these compounds were prepared. The binding studies for **2f** and **2h** were conducted on samples that were dried to constant weight at 50°C and weighed under anhydrous atmosphere in a glove box.

In their classic paper, Clarke and co-workers[29] reported that the addition of (substituted phenyl)magne-sium halides to anhydroecgonine methyl ester (**3**) at −20 °C in diethyl ether, followed by quenching of the reaction in ice after 1 h, gave a 1:3 mixture of the corresponding 3β-(substituted phenyl)tropane-2β-carboxylic acid methyl esters (**2**) and 3β-phenyltropane-2α-carboxylic acid methyl esters (**4**) (Scheme 1). In a reinvestigation of this reaction we showed that conducting the reaction at −40°C and quenching with 2 equiv of trifluoroacetic acid at −78°C in place of ice leads to a higher yield and to selectivity (1.6:1) for the 2β-substituted product.[17] Scheme 1 shows the new analogues prepared by this method, and Table 2 lists the yields and physical properties. The p-hydroxy analogue **2p** was obtained by adding p-methoxymethoxyphenyl magnesium iodide to **3**. The intermediate 3β-(4′-methoxymethoxyphenyl)-tropane-2β-carboxylic acid methyl ester **2z** was treated (without isolation) with 1 N hydrochloric acid at 25°C to give **2p**.

We previously reported[27] that iodination of 3β-(4′-aminophenyl)tropane-2β-carboxylic acid methyl ester (**2f**) with iodine chloride in acetic acid yielded the 3′-iodo-4′-amino analogue **2u**. Diazotization of **2u** followed by treatment of the diazonium salt with hypophospho-rous acid gives the m-iodo analogue **2t**. Bromination of **2f** with N-bromosuccinimide gives the 3′-bromo-4′-amino analogue **2v** (Scheme 2).

Methods

Binding Data. The IC$_{50}$ values for the compounds used in the present study are listed in Table I. Binding data were obtained as previously reported[30] using [^{3}H]-WIN 35,428 as the radioligand. Note that the IC$_{50}$ values for the new samples of **2f** and **2h** are different from those originally reported.[17]

3D-QSAR. Molecular Modeling. All calculations were performed on a Silicon Graphics 4D/310 VGX workstation with the SYBYL[31] (versions 5.41and 6.03) and MOPAC[32] (versions 5.0 and 6.0) software packages. Molecular models of the 3β-(3′-, 4′-, and 3′,4′- substituted phenyl)tropane-2β-carboxylic acid methyl esters were constructed using the X-ray crystallographic coordinates of cocaine[33] and molecular fragments and standard bond
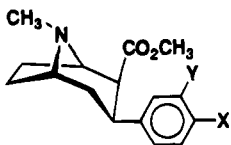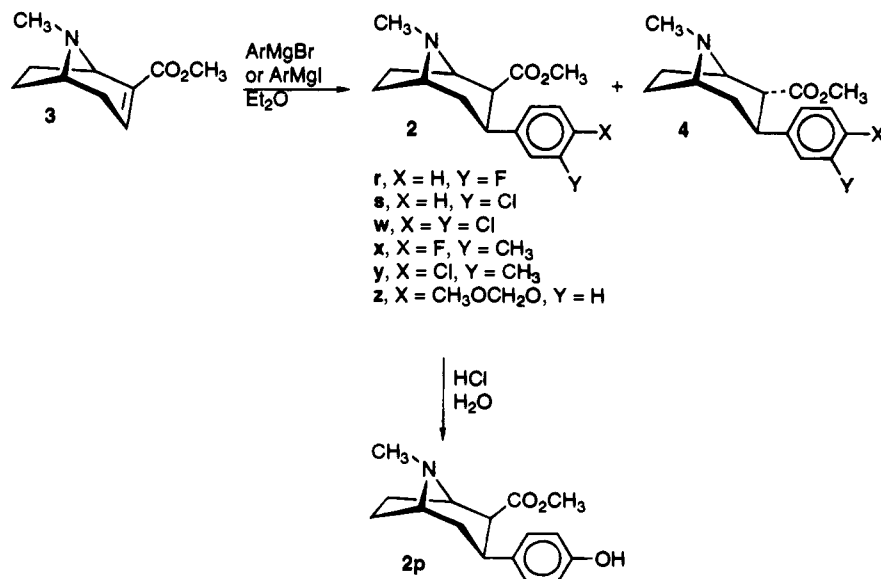
Scheme 1

r, X = H, Y = F
s, X = H, Y = Cl
w, X = Y = Cl
x, X = F, Y = CH$_3$
y, X = Cl, Y = CH$_3$
z, X = CH$_3$OCH$_2$O, Y = H

Table 2. Physical Properties of 3β-(Substituted phenyl)tropane-2β-carboxylic Acid Esters[a]

compd	X	Y	molecular formula[b,c]	yield,[d] %	mp, °C	optical rotation: $[\alpha]^{23}_D$ (c, MeOH)	ArCH₃	NCH₃	OCH₃	H-2	H-3
							selected ¹H NMR[e] resonances				
2p	OH	H	C₂₀H₂₇NO₅[f]	20[g]	173–175	−93.6 (0.11)		2.20	3.49	2.87	2.93
2r	H	F	C₁₆H₂₁ClFNO₂[f]	31	123–125	−113.1 (0.18)		2.90	3.48	2.81	2.97
2s	H	Cl	C₁₆H₂₁Cl₂NO₂[h]	29	111–113	−117.7 (0.27)		2.22	3.42	2.87	2.93
2w	Cl	Cl	C₁₆H₂₀Cl₃NO₂	9[i]	167–168	−115.7 (0.07)		2.38	3.50	3.10	3.45
2x	F	CH₃	C₁₇H₂₃ClFNO₂[h]	29	163–165	−103.8 (0.08)	2.19	2.29	3.49	2.87	2.93
2y	Cl	CH₃	C₁₇H₂₃Cl₂NO₂[j]	5	186–187	−89.5 (0.095)	2.22	2.32	3.51	2.86	2.98

[a] A general procedure for the synthesis of **2r**, **2s**, **2w**, **2x**, and **2y** is given in the Experimental Section. [b] All compounds are hydrochloride salts except **2p** which is a tartrate salt. [c] All compounds were analyzed for C, H, N. The results agreed to ±0.4% with theoretical values. [d] The yields are for the salts recrystallized from a methanol and ether mixture. [e] The ¹H NMR spectra are for the free bases of the compounds. [f] This salt is hydrated with 0.75 mol of water. [g] This is the overall yield for a two-step procedure (see the Experimental Section). [h] This salt is hydrated with 1.5 mol of water. [i] A repeat synthesis of this product gave 65% yield. [j] This salt is hydrated with 2.0 mol of water.

Scheme 2
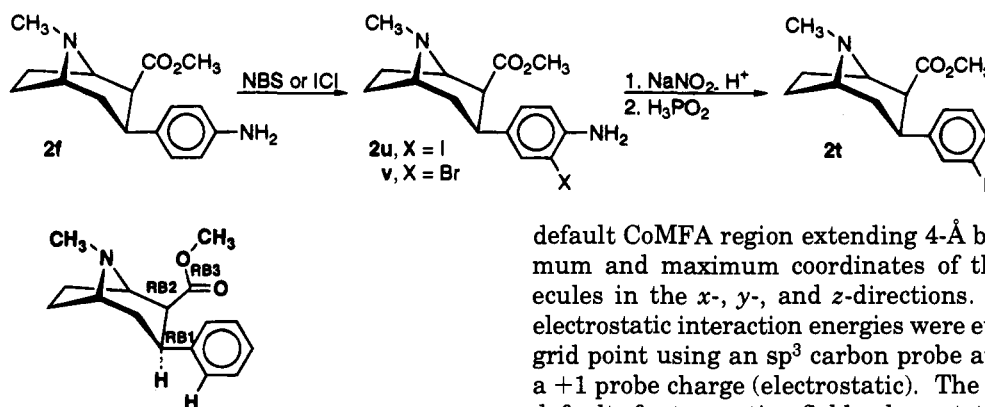
Figure 1. Template structure for CoMFA studies

lengths and angles from the SYBYL structural library. Each structure was optimized using the MAXIMIN2 minimizer (convergence criteria: energy change threshold ≤0.05 kcal/mol). A systematic conformational search at 10° increments was performed on the rotatable bonds RB1 and RB2 of **2a** (Figure 1) using the SYBYL SEARCH module; MAXIMIN2 steric energies were used to identify the global minimum energy conformation. While it is recognized that this conformation may not necessarily be adopted by **2a** in the drug–receptor complex, the use of a reasonable low-energy conformation as a template is a useful starting point for statistical comparisons of flexible structures within the SYBYL CoMFA module.[34] The remaining 3'-, 4'-, and 3',4'-substituted analogues (**2b-y**) were constructed from the **2a** template and energy minimized using MAXIMIN2. All structures were submitted to a final geometry optimization and charge calculation using the AM1 Hamiltonian method[35] in the semiempirical quantum mechanics program MOPAC (keywords: AM1, XYZ, and MMOK). In preparation for 3D-QSAR analysis all structures were aligned by a rigid body least-squares fit of the six aromatic carbon atoms of each compound to the **2a** template.[36]

CoMFA Analysis. All analyses were conducted using program default values. Thus, CoMFA field values were calculated for each structure placed in a region defined by grid points at 2-Å intervals within the

default CoMFA region extending 4-Å beyond the minimum and maximum coordinates of the aligned molecules in the x-, y-, and z-directions. The steric and electrostatic interaction energies were evaluated at each grid point using an sp³ carbon probe atom (steric) and a +1 probe charge (electrostatic). The SYBYL CoMFA defaults for truncating field values at ±30 kcal/mol and dropping electrostatic field values at grid points where the steric field value exceeded 30 kcal/mol were used.

Preliminary full cross-validated partial least-squares (PLS) analyses with the number of cross-validation groups equal to the number of structures in the study (either 12 or 25) and with one to five components were performed to establish the optimum number of components for the best predictive model [i.e., the minimum number of components corresponding to a q^2 ("predictive r^2")[34] within 5% of the maximum q^2]. An analysis was then performed using the optimum number of components to obtain the final PLS model. Conventional r^2 values (r^2_{fit}),[37] F statistic, standard error of estimate (s_{fit}), the relative contribution of the steric and electrostatic CoMFA field terms, and the actual − predicted residuals were determined using this final PLS-derived regression.

The steric and electrostatic features of the final CoMFA model were displayed as contour plots of the PLS regression coefficients at each CoMFA region grid point. The steric CoMFA contributions (STDEV*-COEFFICIENTS option) were contoured at the 75% and 25% levels, with the "positive" steric contour (75%) colored green and the "negative" steric contour (25%) colored yellow. The electrostatic contribution contours were displayed in similar fashion with red-colored "positive" contours (i.e., interaction of ligands with the positive probe atom in these regions enhances activity) at the 75% level and blue-colored "negative" contours

Table 3. Comparison of the Statistical Parameters Derived for QSAR Models

	CoMFA				Hansch	
	model A^a	model $B^{b,c}$	model $C^{b,d}$	model D		
n^e	12	12	12	25	12	25
$q^{2\,f}$	0.545	0.760	0.769	0.733		
$r^2_{fit}{}^g$	0.946	0.940	0.934	0.958	0.835	0.596
$s_{fit}{}^h$	0.212	0.231	0.243	0.166	0.382	0.505
$n_{comp}{}^i$	3	3	3	4		
F	47	41.60	39.59	115.44	13.5	10.3

^{a} Analysis from ref 17. ^{b} CoMFA models derived from IC_{50} values in Table 1. ^{c} The nitrogen lone pair for analogue **2f** is oriented toward the viewer (i.e., the same as in analysis A). ^{d} The nitrogen lone pair is oriented away from the viewer. ^{e} Total number of compounds in the analysis. ^{f} Squared correlation coefficient of a cross-validated analysis. ^{g} Squared correlation coefficient of non-cross-validated analysis. ^{h} Standard deviation of a non-cross-validated analysis. ^{i} Optimum number of PLS components. (For definitions of statistical parameters, see refs 34 and 37.)

(ligand interaction with the positive probe atom in these regions lowers activity) at the 25% level. The steric and electrostatic interactions of individual structures with the final CoMFA model were examined by extracting the CoMFA field of each compound and then contouring the product of these individual fields and the PLS regression coefficients (FIELD*COEFFICIENTS option).

Classical QSAR. Multiple linear regressions were performed using the SAS JMP[38] software package on a Macintosh][cx microcomputer. A QSAR equation was derived using values of the hydrophobic parameter π and of the molar refractivity obtained from the literature,[39-41] or calculated using the MEDCHEM[42] software package, as the independent variables and $-\log(IC_{50})$ as the dependent variable.

Results

In our previous study, we showed that the CoMFA model derived from the potencies of the 12 analogues **2a-l** to inhibit [^{3}H]WIN 35,428 binding at the dopamine transporter provided excellent cross-validated q^2 indicating high predictive capacity (see model A, Table 3). Using the updated IC_{50} values in Table 2 for analogues **2a-l**, with the structures and alignment presented in the methods section, two new models were derived. These are designated models B and C in Table 3. In model C the electron lone pair on the aryl amino group of **2f** is oriented 180° opposite from its position in models A and B. A comparison of the three models shows that q^2 for both new models (B and C) is significantly higher than for the original model (A), while the r^2_{fit} and s_{fit} values are not significantly different. It was determined that including π as an additional PLS variable did not lead to a significant improvement in the CoMFA. The relative steric and electrostatic contributions to the three models (A-C) are essentially identical (see Table 4). Overall, models B and C were the same. CoMFA model B was used to predict the $-\log(IC_{50})$ values of **2m-y** (Table 5, training set). The 4'-substituted analogues **2m** (X = CH$_3$O), **2n** (X = N$_3$), and **2p** (X = HO) were predicted quite well; however, **2o**, which has a 4'-ethyl substituent, was poorly predicted (actual $-\log(IC_{50}) = -1.74$, predicted $= -0.58$). The possibility that the overestimate of the activity of **2o** (by a factor of ~15) is the result of the particular conformation of the ethyl

Table 4. Comparison of the Relative Contribution of Steric and Electrostatic Factors to the CoMFA Models A–D from Table 3

	relative contribution	
CoMFA model	steric	electrostatic
A	0.630	0.380
B	0.623	0.377
C	0.680	0.320
D	0.728	0.272

Table 5. Inhibition Data $[-\log(IC_{50})]$ and QSAR Predictions: CoMFA vs Classical

		CoMFA		Hansch	
compd	actual	predicted	residual	predicted	residual
		Training Set			
2k	−0.10	−0.22	0.12	−0.44	0.34
2d	−0.23	−0.27	0.04	−0.23	0.00
2j	−0.23	−0.29	0.06	−0.48	0.24
2c	−0.49	−0.40	−0.09	−0.38	−0.11
2f	−0.99	−0.60	−0.39	−1.32	0.33
2l	−1.11	−0.83	−0.28	−0.38	−0.74
2e	−1.12	−1.06	−0.06	−0.78	−0.34
2b	−1.14	−1.17	0.03	−1.27	0.13
2a	−1.36	−1.52	0.15	−1.31	−0.05
2g	−1.81	−1.70	−0.10	−1.53	−0.27
2h	−2.08	−2.06	−0.02	−2.22	0.14
2i	−2.50	−2.62	0.12	−2.39	−0.11
rms deviation			0.16		0.30
		Test Set			
2w	0.10	−0.48	0.58	−0.19	0.29
2y	0.09	−0.29	0.38	−0.10	0.20
2u	−0.13	−0.53	0.40	−1.89	1.76
2n	−0.33	−0.63	0.30	−0.44	0.12
2x	−0.47	−1.12	0.65	−0.31	−0.16
2v	−0.59	−0.65	0.06	−1.03	0.43
2s	−0.80	−1.67	0.88	−0.38	−0.41
2m	−0.96	−0.72	−0.24	−0.64	−0.32
2p	−1.08	−0.82	−0.26	−1.34	0.25
2r	−1.22	−1.74	0.52	−1.27	0.05
2t	−1.42	−1.47	0.05	−0.44	−0.98
2o	−1.74	−0.58	−1.16	−0.19	−1.55
2q	−2.16	−1.37	−0.79	−5.34	3.18
rms deviation			0.58		1.15

group selected for the CoMFA prediction was examined by calculating the predicted activity of the 4'-ethyl conformers of **2o** at 5° increments from 0 to 360°. The maximum predicted value determined in this manner was −0.727 (or an IC_{50} of 5.33 nM) and the minimum was −0.283 (IC_{50} of 1.92 nM). Thus, it appears that the larger part of the error in the prediction of the potency of the 4'-ethyl derivative is not associated with the choice of conformation in this case. The model also predicted a much lower $-\log(IC_{50})$, −1.37, for the 4'-trimethylstannyl analogue **2q** than the experimental value of −2.16. The potency of the 3'-iodo analogue **2t**, with $-\log(IC_{50})$ values of −1.42 and −1.47 for experimental and predicted values, respectively, was quite accurately predicted, while the values for 3'-fluoro and 3'-chloro analogues, **2r** and **2s**, respectively, were more poorly predicted. The model did reasonably well in predicting the $-\log(IC_{50})$ values of the disubstituted analogues **2v-y**.

A CoMFA study was conducted using all 25 analogues listed in Table 1. The three aromatic amino compounds, **2f**, **2u**, and **2v**, were included in conformations with the lone pair of the amino nitrogen in either of its two possible conjugated orientations. Similarly, two conformations in which the lone pair electrons were in conjugation with the aromatic ring were included for
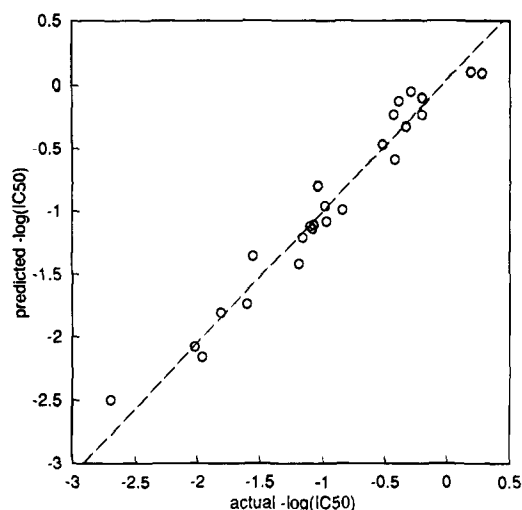
Figure 2. Predicted vs experimental $-\log(IC_{50})$ values for inhibition of [^{3}H]WIN 35,428 binding to the dopamine transporter for 25 cocaine analogs (model D).

the p-methoxy (**2m**) and p-hydroxy (**2p**) analogues; four conformations were included for the p-ethyl (**2o**) analogue. The CoMFA for several combinations of conformations of these analogues exhibited strong cross-validated correlations indicating that they were highly predictive. The q^2 for the analysis varied from 0.506 (three components) to 0.733 (four components). The observation that all combinations of conformations evaluated gave statistically valid analyses provides confidence that, in this case, the predictive power of CoMFA is relatively independent of the selection of side-chain conformation. Table 3 lists the statistical results derived from the best CoMFA model (model D), and the relative contribution of steric and electrostatic factors in this model is listed in Table 4. Evidence for the predictive potential of CoMFA model D is provided in Figure 2 which shows a plot of actual versus predicted $-\log(IC_{50})$ values.

Dr. Hansch[43] brought to our attention that a conventional QSAR analysis of 14 of the compounds, **2a-n**, used in our original study[17] (12 that we used for CoMFA and two for prediction) gave a satisfactory correlation of π, MR, and $(MR)^2$ with $-\log(IC_{50})$ in a multiple linear regression analysis. The Hansch QSAR analysis of **2a-l** (the compounds studied in the original CoMFA)[17] using the same terms, gave eq 1. The statistical data obtained using the Hansch analysis are shown in Table 3.

$$\log 1/IC_{50} = 0.46\pi + 0.20MR - 0.01(MR)^2 - 1.51$$
$$(1)$$

The ability of a Hansch QSAR analysis (using the π and MR molecular descriptors) to reproduce the data of the entire set of 25 compounds was also evaluated. The r^2 and s_{fit} values derived from this data set was not as good as that obtained from the original 12-compound study (Table 3).

The relative abilities of the three-component CoMFA model B and the Hansch QSAR equation based on π and MR (eq 1) to predict $-\log(IC_{50})$ values for a test set of 13 additional compounds, **2m-y**, are shown in Table 5. The ability of each QSAR model to reproduce the original data (compounds **2a-l**) is also compared in this table. The root-mean-square (rms) deviation of the CoMFA model fit to the original data is 0.16 compared

to 0.30 for the classical QSAR equation. Not unexpectedly, both models perform less well in predicting the $-\log(IC_{50})$ of the test set of 13 compounds which contain substituents and substitution patterns not present in the original 12-compound training set. The CoMFA 3D-QSAR method provides an rms deviation of predictions of 0.58 as compared to 1.15 for predictions based on the classical QSAR equation. Eliminating the trimethyltin derivative (**2q**), whose π parameter is significantly less well-parameterized, improves the performance of both QSAR models but has a larger effect on the classical model, yielding a CoMFA rms of 0.55 and a classical QSAR rms of 0.77.

The results of the CoMFA are conveniently viewed as color-coded contour plots (Figure 3). These contours represent the lattice points where differences in field values are associated with differences in binding affinity. The major steric features of the CoMFA-derived models B and D are compared in Figure 3i and 3iii, respectively, in the form of contour maps, displayed as shaded surfaces. The surfaces indicate regions near the template molecule (**2a**) where increase (green region) or decrease (yellow) in steric bulk would be important. Comparison of the positive and negative steric regions of the 12-compound model B to those of the 25-compound model D shows that they have very similar features.

The electrostatic features of the 12- and 25-compound CoMFA models are illustrated in Figure 3ii and 3iv. The "positive" electrostatic region (colored blue) encloses CoMFA region grid points where the presence of a $+1$ probe charge is linked to increased activity. Likewise, the "negative" electrostatic region (red) defines areas where the $+1$ probe charge is associated with decreased activity. For the purposes of a QSAR study, the receptor is usually conceived to be a fixed environment into which various ligands are introduced. It is therefore useful to interpret the electrostatic CoMFA contours in terms of what they imply about the effect of altering ligand electronegativity via substitution. Thus, increasing the electronegativity of the ligand adjacent to the "positive" (blue) or decreasing the electronegativity of the ligand adjacent to the "negative" (red) electrostatic CoMFA regions is predicted to increase the activity of the ligand.

Discussion

Investigations of the effects of structure modifications of cocaine on its potency at the dopamine transporter have shown that only changes at the 3-position have led to higher potency analogues.[6,17-23] Therefore, we selected modification of the substitution pattern of the phenyl group of **2a** as the starting point for development of a pharmacophore for the cocaine binding site at the dopamine transporter. Examination of the IC_{50} values in Table 1 for compounds **2a-y** reveals that substitution of the 4'-position of **2a** with a chloro, bromo, iodo, or methyl group (**2c, 2d, 2k,** and **2j**) provides compounds with IC_{50} values less than 2 nM. 4'-Substitution with electron-withdrawing nitro and trifluoromethyl groups (compounds **2e** and **2l**) or electron-donating amino, methoxy, and hydroxy groups (compounds **2f, 2m,** and **2p**) provides compounds with similar IC_{50} values, 1 order of magnitude less potent than **2c, 2d, 2k,** and **2j**. Large 4'-substituents such as acetylamino, propionyl-
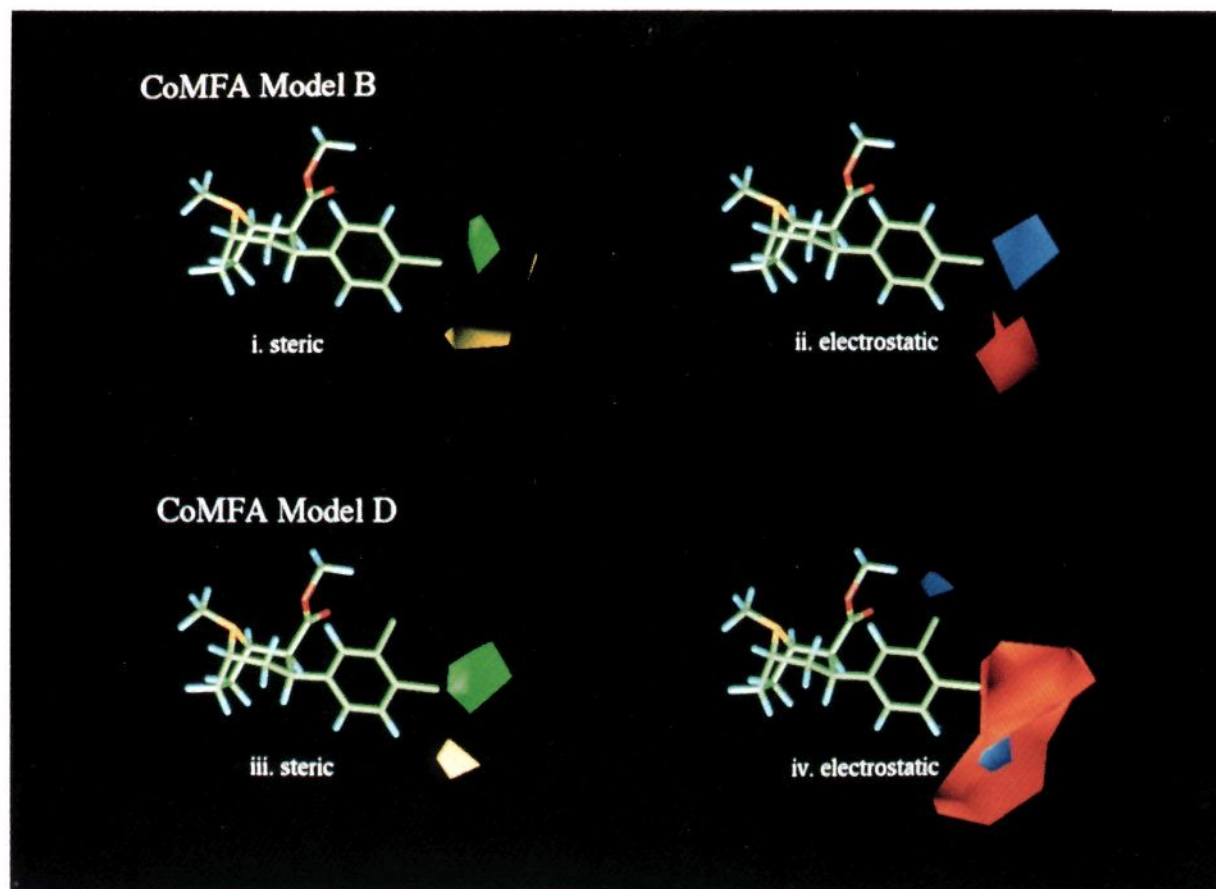
Figure 3. Overlay of structure **2a** and 12-compound model B CoMFA steric map (3i) and 25-compound model D CoMFA steric map (3ii). Green contours (level 75%) surround regions where steric bulk enhances binding. Yellow contours (level 25%) encompass regions where steric bulk decreases binding. Overlay of structure **2a** and 12-compound model B CoMFA electrostatic map (3iii) and 25-compound model D CoMFA electrostatic map (3iv). Red contours (level 75%) show region where positive probe atom is associated with increased affinity and blue contours (level 25%) show regions where the positive probe decreased affinity.

amino, (ethoxycarbonyl)amino, and trimethylstannyl resulted in compounds (**2g-i**, and **2q**) with low affinity for the DA transporter. Surprisingly, the 4′-ethyl analogue **2o**, which is only slightly larger than the 4′-methyl analogue **2j**, *is 32 times less potent*. Substitution at the 3′-position had somewhat inconsistent results; 3′-substitution of **2a** resulted in analogues (**2r-t**) with lower affinity than the corresponding 4′-substituted counterparts, while the addition of a 3′-chloro or 3′-methyl group to analogue **2c**, to give the 3′,4′-dichloro and 4′-chloro-3′-methyl analogues, **2w** and **2y**, respectively, had only a minor effect on potency. Strikingly, the addition of a 3′-methyl group to the 4′-fluoro analogue **2b** or a 3′-bromo or 3′-iodo substituent to the 4′-amino analogue **2f** increased potency relative to the 4′-substituted analogue.

The capacity to design new biologically active compounds on the basis of previously synthesized and tested compounds is an aid in drug design. Traditional QSAR studies have been used since the early 1970s[40] to correlate and predict biological activities of untested molecules. More recently, 3D QSAR techniques like CoMFA have shown promise of extending the QSAR method. In this method, a suitable sampling of the steric and electrostatic field around a set of aligned structures provides information required for predicting the activity of untested structures. A comparison of the classical and CoMFA approaches was recently reviewed.[44]

We had previously found that whereas classical QSAR failed to show high intercorrelation for a subset of the compounds in this investigation, CoMFA gave satisfactory agreement between experimental and predicted IC_{50} values.[17] *Comparison of predicted* $-log(IC_{50})$ *values of* several new analogues, obtained by using the CoMFA model B (12-compound model) and by using the Hansch model, with experimental $-log(IC_{50})$ values (Table 5) shows that lower rms deviations are obtained from the CoMFA model than from the classical (or extrathermodynamic) QSAR model for both the 12-compound "training" set and the 13-compound "test" set. Results from our early study,[17] as well as from the present study, show that both methods indicate statistically a minor electrostatic contribution to the binding affinity.

In our previously reported 12-compound CoMFA model[17] (model A), which was based on 4′-substituted phenyl analogues, we reported that the steric field contour map showed a positive region extending out from and slightly above the 4′-position and a negative region further out from and below the 4′-position. As expected, the new 12-compound model (model B) shows the same features. These positive and negative steric regions are shown as green and yellow translucent contours in Figure 3i. The 25-compound model (model D), which is based on analogues with 4′-, 3′-, and 3′,4′-substituents, shows a steric field contour map, Figure 3iii, very similar to the model B map (Figure 3i), even though it includes compounds with steric groups in

regions not included in models A and B. The only difference between the maps is that both the positive (green) and negative (yellow) regions of model D are slightly larger than the corresponding regions in model B.

The FIELD*COEFFICIENT contour plots generated from individual compound and the PLS-model electrostatic CoMFA fields (Figure 3ii and 3iv) were examined to assess the electrostatic influence of the various substitution patterns. For the original 12-compound model, these contour plots suggest that negative electrostatic potential presented by ligands above and below the plane of the aromatic ring and in the vicinity of the carbonyl oxygens of the 2β-carbomethoxy- and 4'-substituents is associated with enhanced potency. Increasing positive electrostatic potential at the edge of the phenyl ring, particularly in the region directly between the phenyl ring and the methyl group of the 2-position ester, can also be seen to be associated with higher potency. The 25-compound model (D) exhibits many of the same electrostatic features but suggests that increased electron density around both the aromatic ring and the 4'-substituent itself is associated with higher potency.

The correlation ($r^2 = 0.958$) provided by the CoMFA technique on the full 25-compound set is somewhat higher than that obtained from the 12-compound models ($r^2 = 0.946, 0.940,$ and 0.934). The residuals of the calculated activities of the ethyl and trimethylstannyl derivatives, which were large using CoMFA models A, B, and C, are significantly smaller using the CoMFA model D. For the ethyl derivative, the predicted residual (model B) was -1.16, while the calculated residual (model D) is -0.137. A similar trend is found for the trimethylstannyl derivative with a predicted residual (model B) of -0.79 and a calculated residual (model D) of -0.20. In contrast, the classical QSAR in which, although the 25-compound analysis provides significantly lower residuals for the calculated values of the 4'-trimethylstannyl derivative (predicted residual 3.18, calculated residual 0.27), a significantly lower overall correlation ($r^2 = 0.60$) was obtained, did not greatly improve the calculated residual of the problematic 4'-ethyl derivative (predicted residual -1.55, calculated residual -1.16). For this group of compounds, the CoMFA technique provides a consistent improvement in overall correlation and accuracy in the estimation of the activity of individual compounds as more compounds are included in the calculations, while the classical QSAR correlation does not uniformly improve as more compounds are included in the multiple linear regression. While the classical QSAR may possibly be improved by including more or different molecular descriptors in the regression equation, the CoMFA technique, relying only on default program parameters and the calculated steric and electrostatic fields, rapidly and flexibly provides useful correlations and predictions. On the other hand, the classical QSAR model suggests that the distribution property (π) is important.

Conclusion

Several new 3β-(substituted phenyl)tropane-2β-carboxylic acid methyl esters described in this study provided new SAR information on the cocaine binding site pharmacophore. Surprisingly, the 3β-(4'-ethylphe-

nyl) analogue **2a** was 32 times less potent than the 3β-(4'-methylphenyl) analogue **2i**. In addition, 3β-(3'-halophenyl) analogues were less potent than the corresponding 3β-(4'-halophenyl) derivatives, and more important, several 3β-(3',4'-disubstituted phenyl) analogues were equal to or more potent than the 3β-(4'-substituted phenyl) analogues.

The classical QSAR model shows that compound-specific distribution properties (hydrophobicity) are important contributors to binding affinity at the DA transporter while the CoMFA approach effectively correlates and predicts the effect of aromatic substitution on binding affinity. Furthermore, since the CoMFA results are independent of the conformation of aromatic substituents selected for modeling, CoMFA may have wide applications. The new CoMFA model derived from 25 compounds (model D) shows that some steric bulk extended from and above the 4'-position contributes to enhanced potency while excessive bulk leads to reduced potency. In addition, the model suggests that although electrostatic forces account for only 27% of the binding affinity, they may make a significant contribution to potency.

Model D will have utility in the design of third-generation, high-affinity ligands for the DA transporter. More important, since our goal is to develop ligands selective for all three monoamine transporters, we are presently determining the IC$_{50}$ values for the same 25 compounds for binding the 5-HT and NE transporters. We expect that a comparsison of CoMFA models for all three transporters will be useful for the design of 5-HT and NE selective binding ligands.

Experimental Section

Melting points were determined on a Thomas-Hoover capillary tube apparatus. All optical rotations were determined at the sodium D line using a Rudolph Research Autopol III polarimeter (1 dm cell). NMR spectra were recorded on a Bruker WM-250 or AM-500 spectrometer using tetramethylsilane as internal standard. Thin-layer chromatography was carried out on Whatman silica gel 60 plates using hexane:Et$_2$O: Et$_3$N (10:9:1). Visualization was accomplished under UV or in an iodine chamber. Since all the compounds described were prepared starting from natural cocaine, they are all optically active and have the absolute configuration of natural cocaine. Microanalyses were carried out by Atlantic Microlab, Inc. Cocaine was provided by the National Institute on Drug Abuse. [^{3}H]-3β-(p-Fluorophenyl)tropane-2β-carboxylic acid methyl ester ([^{3}H]WIN 35,428) was purchased from Dupont-New England Nuclear (Boston, MA).

General Procedure for Preparing 3β-(Substituted phenyl)tropane-2β-carboxylic Acid Methyl Ester (2) from Anhydroecgonine Methyl Ester 3. Compounds **2r-s** and **2w-y** were synthesized using procedures analogous to those reported for similar compounds.[23] Physical data are given in Table 2.

3β-(4'-Hydroxyphenyl)tropane-2β-carboxylic Acid Methyl Ester (2p) Tartrate. To a flask containing [p-(methoxymethoxy)phenyl] magnesium iodide (11.0 mmol) in Et$_2$O (125 mL) at -55 °C was added **3** (0.50 g, 5.52 mmol). The suspension was stirred for 3 h before cooling to -78°C and adding CF$_3$CO$_2$H (2 mL). The resulting solution was stirred an additional 2 h before adding 6 N HCl (50 mL). The reaction mixture was washed with Et$_2$O (3 × 100 mL). The aqueous layer was basified (pH 9) and extracted with CHCl$_3$ (3 × 50 mL). The combined organic layers were concentrated under reduced pressure. Without further purification, the crude residue was dissolved in 1 N HCl and stirred overnight at ambient temperature. The crude reaction mixture was basified and extracted with CHCl$_3$ (3 × 25 mL). The combined

organic extract was dried (MgSO₄) and evaporated under reduced pressure to yield the crude product. The product was separated by flash chromatography on SiO₂ (9:2 Et₂O–Et₃N). The physical constants for **2p** are listed in Table 2.

3β-(3′-Iodophenyl)tropane-2β-carboxylic Acid Methyl Ester (2t) Hydrochloride. To a solution of 3β-(3′-iodo-4′-aminophenyl)tropane-2β-carboxylic acid methyl ester dihydrochloride[27] **2v** (280 mg, 0.70 mmol) in H₃PO₄ (10 mL) was added an aqueous solution of NaNO₂ (50 mg, 0.77 mmol, in 0.5 mL of H₂O) at 0°C. After 30 min at this temperature, H₃PO₂ (12.5 mL, 50%) was added dropwise, and the reaction mixture was stirred for 2 h at room temperature. The reaction mixture was poured into ice-water, basified with concentrated NH₄OH, and extracted with Et₂O. After washing with H₂O, the organic layer was dried over MgSO₄ and concentrated to give an oil which was purified by flash chromatography on SiO₂ (hexane:Et₂O, 4:1); ¹H NMR (250 MHz, CDCl₃) δ 1.52–1.71 (m, 3), 2.03-2.18 (m, 2), 2.23 (s, 3, NCH₃), 2.51 (m, 1), 2.86–2.98 (m, 2), 3.33 (m, 1, H-5), 3.51 (s, 3, OCH₃), 3.55 (m, 1, H-1), 6.90 (t, $J = 7$ Hz, 1, ArH), 7.27 (d, $J = 7$ Hz, 1, ArH), 7.47 (d, $J = 7$ Hz, 1, ArH), 7.76 (s, 1, ArH). The pure free base was converted to the HCl salt to yield 154 mg (52%) of **2t·HCl** as a white solid: mp 138–140°C; $[\alpha]^{25}_{D}$ −91.6° (c 0.25 CH₃OH). Anal. Calcd for C₁₆H₂₀ClINO₂·0.75H₂O: C, H, N.

3β-(3′-Bromo-4′-aminophenyl)tropane-2β-carboxylic Acid Methyl Ester (2v) Dihydrochloride. To a round-bottomed flask containing DMF (2.5 mL) under a stream of nitrogen gas at ambient temperature was added 3β-(4′-aminophenyl)tropane-2β-carboxylic acid methyl ester (**2f**) (100 mg, 0.364 mmol) and NBS (64.5 mg, 0.364 mmol). The solution immediately turned deep red. After the solution was stirred for 2.5 h, H₂O (5 mL) was added, and the reaction mixture was extracted with CHCl₃ (2 × 25 mL). The combined organic extract was dried (MgSO₄) and concentrated under reduced pressure to yield the crude product as a brown oil. Flash chromatography on SiO₂ (5% CH₃OH in CHCl₃) afforded 42 mg (33%) of pure product **2v** as a yellow oil. The hydrochloride salt had the following properties: mp 194 °C dec; $[\alpha]^{25}_{D}$ −87.7° (c 0.09, CH₃OH); partial ¹H NMR (250 MHz, DMSO) δ 2.28 (s, 3, NCH₃), 3.52 (s, 3, OCH₃), 7.96–8.68 (m, 3). Anal. Calcd for C₁₆H₂₃BrCl₂N₂O₂·2H₂O: C, H, N.

Ligand Binding. Brains from male Sprague–Dawley rats weighing 200–250 g (Harlan Labs, Indianapolis, IN) were removed, dissected, and rapidly frozen. Ligand binding experiments for the dopamine transporter were conducted in assay tubes containing 0.5 mL of buffer (10 mM sodium phosphate containing 0.32 M sucrose, pH 7.40) on ice for 120 min. Each assay tube contained 0.5 nM [³H]WIN 35,428 and 0.1 mg of striatal tissue (original wet weight). The nonspecific binding was defined using 30 μM (−)-cocaine. Results were analyzed using the Equilibrium Binding Data Analysis software (EBDA, Biosoft).

References

(1) Reith, M. E. A.; Shershen, H.; Lajtha, A. Saturable [³H]cocaine binding in central nervous system of mouse. *Life Sci.* **1980**, 27, 1055–1062.

(2) Kennedy, L. T.; Hanbauer, I. Sodium-sensitive cocaine binding to rat striatal membrane: Possible relationship to dopamine uptake sites. *J. Neurochem.* **1983**, 41, 172–178.

(3) Calligaro, D. O.; Eldefrawi, M. E. Central and peripheral cocaine receptors. *J. Pharmacol. Exp. Ther.* **1987**, 243, 61–67.

(4) Madras, B. K.; Fahey, M. A.; Bergman, J.; Canfield, D. R.; Spealman, R. D. Effects of cocaine and related drugs in nonhuman primates. I. [³H]Cocaine binding sites in caudate-putamen. *J. Pharmacol. Exp. Ther.* **1989**, 251, 132-141.

(5) Schoemaker, H.; Pimoule, C.; Arbilla, S.; Scattom, B.; Javoy-Agid, F.; Langer, S. W. Sodium dependent [³H]cocaine binding associated with dopamine uptake sites the rat striatum and human putamen decrease after dopaminergic denervation and in Parkinson's disease. *Naunyn. Schmiedebergs Arch. Pharmacol.* **1985**, 329, 227–235.

(6) Carroll, F. I.; Lewin, A. H.; Boja, J. W.; Kuhar, M. J. Cocaine receptor: Biochemical characterization and structure-activity relationships for the dopamine transporter. *J. Med. Chem.* **1992**, 35, 969–981.

(7) Kuhar, M. J.; Ritz, M. C.; Boja, J. W. The dopamine hypothesis of the reinforcing properties of cocaine. *Trends Neurosci.* **1991**, 14, 299–302.

(8) Ritz, M. C.; Lamb, R. J.; Goldberg, S. R.; Kuhar, M. J. Cocaine receptors on dopamine transporters are related to self-administration of cocaine. *Science* **1987**, 237, 1219–1223.

(9) Bergman, J.; Madras, B. K.; Johnson, S. E.; Spealman, R. D. Effects of cocaine and related drugs in nonhuman primates. III. Self-administration by squirrel monkeys. *J. Pharmacol. Exp. Ther.* **1989**, 219, 150–155.

(10) Carroll, F. I.; Lewin, A. H.; Abraham, P.; Parham, K.; Boja, J. W.; Kuhar, M. J. Synthesis and ligand binding of cocaine isomers at the cocaine receptor. *J. Med. Chem.* **1991**, 34, 883–886.

(11) Shimada, S.; Kitayama, S.; Lin, C.-L.; Patel, A.; Nanthakumar, E.; Gregor, P.; Kuhar, M.; Uhl, G. Cloning and expression of a cocaine-sensitive dopamine transporter complementary DNA. *Science* **1991**, 254, 576–578.

(12) Kilty, J. E.; Lorang, D. B.; Amara, S. G. Cloning and Expression of a Cocaine-Sensitive Rat Dopamine Transporter. *Science U.S.A.* **1991**, 254, 578–579.

(13) Usdin, T. B.; Mezey, E.; Chen, C.; Brownstein, M. J.; Hoffman, B. J. Cloning of the cocaine-sensitive bovine dopamine transporter. *Proc. Natl. Acad. Sci.* **1991**, 88, 11168–11171.

(14) Giros, B.; Mestikawy, S. E.; Godinot, N.; Zheng, K.; Han, H.; Yang-Feng, T.; Caron, M. G. Cloning, pharmacological characterization, and chromosome assignment of the human dopamine transporter. *Mol. Pharmacol.* **1992**, 42, 383-390.

(15) Reith, M. E. A.; Meisler, B. E.; Sershen, H.; Lajtha, A. Structural requirements for cocaine congeners to interact with dopamine and serotonin uptake sites in mouse brain and to induced stereotyped behavior. *Biochem. Pharmacol.* **1986**, 35, 1123–1129.

(16) Ritz, M. C.; Cone, E. J.; Cone, M. J. Cocaine inhibition of ligand binding at dopamine, norepinephrine and serotonin transporters: A structure-activity study. *Life Sci.* **1990**, 46, 635–645.

(17) Carroll, F. I.; Gao, Y.; Rahman, M. A.; Abraham, P.; Lewin, A. H.; Boja, J. W.; Kuhar, M. J. Synthesis, ligand binding, QSAR, and CoMFA study of 3β-(p-substituted phenyl)tropan-2β-carboxylic acid methyl esters. *J. Med. Chem.* **1991**, 34, 2719–2927.

(18) Meltzer, P. C.; Liang, A. Y.; Brownell, A.-L.; Elmaleh, D. R.; Madras, B. K. Substituted 3-phenyltropane analogs of cocaine: Synthesis, inhibition of binding at cocaine recognition sites, and positron emission tomography imaging. *J. Med. Chem.* **1993**, 36, 855–862.

(19) Davies, H. M. L.; Saikali, E.; Sexton, T.; Childers, S. R. Novel 2-substituted cocaine analogs: Binding properties at dopamine transport sites in rat striatum. *Eur. J. Pharmacol.-Mol. Pharmacol. Sec.* **1993**, 244, 93–97.

(20) Kozikowski, A. P.; Roberti, M.; Xiang, L.; Bergmann, J. S.; Callahan, P. M.; Cunningham, K. A.; Johnson, K. M. Structure-activity relationship studies of cocaine: Replacement of the C-2 ester group by vinyl argues against H-bonding and provides an esterase-resistant, high-affinity cocaine analogue. *J. Med. Chem.* **1992**, 35, 4764–4766.

(21) Kline, R. H., Jr.; Wright, J.; Fox, K. M.; Eldefrawi, M. E. Synthesis of 3-arylecgonine analogues as inhibitors of cocaine binding and dopamine uptake. *J. Med. Chem.* **1990**, 33, 2024–202 .

(22) Carroll, F. I.; Abraham, P.; Lewin, A. H.; Parham, K. A.; Boja, J. W.; Kuhar, M. J. Isopropyl and phenyl esters of 3β-(4-substituted phenyl)tropan-2β-carboxylic acids. Potent and selective compounds for the dopamine transporter. *J. Med. Chem.* **1992**, 35, 2497–2500.

(23) Carroll, F. I.; Kuzemko, M. A.; Gao, Y.; Abraham, P.; Lewin, A. H.; Boja, J. W.; Kuhar, M. J. Synthesis and ligand binding of 3β-(3-substituted phenyl)- and 3β-(3,4-disubstituted phenyl)-tropane-2β-carboxylic acid methyl esters. *Med. Chem. Res.* **1992**, 1, 382–387.

(24) Carroll, F. I.; Gray, J. L.; Abraham, P.; Kuzemko, M. A.; Lewin, A. H.; Boja, J. W.; Kuhar, M. J. 3-Aryl-2-(3′-substituted-1′,2′,4′-oxadiazole-5′-yl)tropane analogues of cocaine: Affinities at the cocaine binding site at the dopamine, serotonin, and norepinephrine transporters. *J. Med. Chem.* **1993**, 36, 2886–2890.

(25) Good, A. C.; Peterson, S. J.; Richards, W. G. QSAR's from similarity matrices. Technique validation and application in the comparison of different similarity evaluation methods. *J. Med. Chem.* **1993**, 36, 2929–2937.

(26) Srivastava, S.; Crippen, G. M. Analysis of cocaine receptor site ligand binding by three-dimensional Voronoi site modeling approach. *J. Med. Chem.* **1993**, 36, 3572–3579.

(27) Carroll, F. I.; Gao, Y.; Abraham, P.; Lewin, A. H.; Lew, R.; Patel, A.; Boja, J. W.; Kuhar, M. J. Probes for the cocaine receptor. Potentially irreversible ligands for the dopamine transporter. *J. Med. Chem.* **1992**, 35, 1813–1817.

(28) Boja, J. W.; Kuhar, M. J.; Kopajtic, T.; Yang, E.; Abraham, P.; Lewin, A. H.; Carroll, F. I. Secondary amine analogues of 3β-(4'-substituted phenyl)tropane-2β-carboxylic acid esters and *N*-norcocaine exhibit enhanced affinity for serotonin and norepinephrine transporters. *J. Med. Chem.* **1994**, *37*, 1220−1223.

(29) Clarke, R. L.; Daum, S. J.; Gambino, A. J.; Aceto, M. D.; Pearl, J.; Levitt, M.; Cumiskey, W. R.; Bogado, E. F. Compounds affecting the central nervous system. 4. 3β-Phenyltropane-2-carboxylic esters and analogs. *J. Med. Chem.* **1973**, *16*, 1260−1267.

(30) Boja, J. W.; Rahman, M. A.; Philip, A.; Lewin, A. H.; Carroll, F. I.; Kuhar, M. J. Isothiocyanate derivatives of cocaine: Irreversible inhibition of ligand binding at the dopamine transporter. *Mol. Pharmacol.* **1991**, *39*, 339−345.

(31) SYBYL, Version 6.0, Tripos Associates, Inc., 1699 S. Hanley Rd., Suite 303, St. Louis, MO 63144−2913, 1992.

(32) MOPAC, Version 6.0 (QCPE No. 455), Quantum Chemistry Program Exchange, Indiana University, Creative Arts Building 181, Bloomington, IN 47405, 1990.

(33) Hrynchuk, R. J.; Barton, R. J.; Robertson, B. E. The crystal structure of free base cocaine, $C_{17}H_{21}NO_4$. *Can. J. Chem.* **1983**, *61*, 481−487.

(34) Cramer, R. D., III; DePreist, S. A.; Patterson, D. E.; Hecht, P. The developing practice of comparative molecular field analysis. In *3D QSAR in Drug Design−Theory, Methods and Applications*; Kubinyi, H., Ed.; ESCOM: Leiden, 1993; pp 443−485.

(35) Dewar, M. J. S.; Zoebish, E. G.; Healy, E. F.; Stewart, J. J. P. AM1: A new general purpose quantum mechanical molecular model. *J. Am. Chem. Soc.* **1985**, *107*, 3902−3909.

(36) Coordinates of all compounds are available on request as SYBYL MOL2 files on Macintosh 3.5-in. high-density disks.

(37) Thibaut, U. Applications of CoMFA and Related 3D QSAR Approaches. In *3D QSAR in Drug Design−Theory, Methods and Applications*; Kubinyi, H., Ed.; ESCOM: Leiden, 1993; pp 661−696.

(38) JMP, Version 2.0, SAS Institute Inc., Cary, NC 27513, 1991.

(39) Hansch, C.; Steward, A. R.; Anderson, S. M.; Bentley, D. The parabolic dependence of drug action upon lipophilic character as revealed by a study of hypnotics. *J. Med. Chem.* **1968**, *11*, 1−11.

(40) Hansch, C.; Leo, A. J.; Unger, S. H.; Kim, K. H.; Nikaitani, D.; Lien, E. J. "Aromatic" substituent constants for structure-activity correlations. *J. Med. Chem.* **1973**, *16*, 1207−1222.

(41) Hansch, C.; Unger, S. H.; Forsythe, A. B. Strategy in drug design. Cluster analysis as an aid in the selection of substituents. *J. Med. Chem.* **1973**, *16*, 1217−1222.

(42) MEDCHEM, Version 3.53, Daylight Chemical Information Systems, Inc., 18500 Von Karman Ave., Irvine, CA 92715, 1988.

(43) Dr. Corwin Hansch, personal communication.

(44) Kim, K. H. Comparison of classical and 3D QSAR. In *3D QSAR in Drug Design−Theory, Methods and Applications*; Kubinyi, H., Ed.; ESCOM: Leiden, 1993; pp 619−642.